Fossil palm beetles refine upland winter temperatures in the Early Eocene Climatic Optimum

S. Bruce Archibald[a,b,c,1], Geoffrey E. Morse[d], David R. Greenwood[e,f], and Rolf W. Mathewes[a]

[a]Department of Biological Sciences, Simon Fraser University, Burnaby, BC, Canada V5A 1S6; [b]Royal British Columbia Museum, Victoria, BC, Canada V8W 1A1; [c]Entomology Department, Museum of Comparative Zoology, Cambridge, MA 02138; [d]Biology Department, University of San Diego, San Diego, CA 92110; [e]Biology Department, Brandon University, Brandon, MB, Canada R7A 6A9; and [f]Barbara Hardy Institute, University of South Australia, Adelaide, SA 5000, Australia

Edited by Thure E. Cerling, University of Utah, Salt Lake City, UT, and approved April 11, 2014 (received for review December 16, 2013)

Eocene climate and associated biotic patterns provide an analog system to understand their modern interactions. The relationship between mean annual temperatures and winter temperatures—temperature seasonality—may be an important factor in this dynamic. Fossils of frost-intolerant palms imply low Eocene temperature seasonality into high latitudes, constraining average winter temperatures there to >8 °C. However, their presence in a paleocommunity may be obscured by taphonomic and identification factors for macrofossils and pollen. We circumvented these problems by establishing the presence of obligate palm-feeding beetles (Chrysomelidae: Pachymerina) at three localities (a fourth, tentatively) in microthermal to lower mesothermal Early Eocene upland communities in Washington and British Columbia. This provides support for warmer winter Eocene climates extending northward into cooler Canadian uplands.

palm bruchines | paleoclimate | Okanagan Highlands | palm pollen

Eocene climates have received intense scrutiny in recent decades, providing an increasingly detailed analog system with which to assess the dynamics of modern global climate change, thereby allowing prediction of its long-term trends and biotic consequences. It was a time of increased global temperatures associated with elevated atmospheric carbon levels, particularly during episodic hyperthermal events such as the Early Eocene Climatic Optimum (EECO) (1, 2). The Eocene was also notable for greater climatic homogeneity, with low latitudinal temperature gradients coupled with low temperature seasonality extending to the poles, creating a global climate type unknown today outside of restricted regions. This is thought to have had far-ranging biological consequences, e.g., for intercontinental dispersal, global biodiversity patterns, community structures, and evolutionary trajectories (e.g., refs. 2–6). Here, we use the presence of insects that have obligate associations with floral climatic indicators to refine characterization of winter climate in a cool higher midlatitude upland during the EECO, and therefore the environmental context of these biotic patterns during an interval of global warmth.

A key factor in these dynamics may have been warmer winter temperatures [coldest month mean temperature (CMMT)] relative to mean annual temperature (MAT) even in mid- and higher latitude regions of cooler MAT (3). Consequently—as in the modern tropics and some southern hemisphere midlatitude coastal areas—Eocene organisms across the globe would not have been burdened by the necessity to allocate resources to endure hostile extreme winter climates with its costs for metabolic and insulation adaptations, or escape its effects by an annual period of dormancy or expenditure of large amounts of energy in migration. This would allow the potential of near year-round reproduction, feeding, and growth, providing an explanatory context for observed differential Eocene diversity patterns. In the geologically brief time scale of our modern interval of global climate change, the partial release of such constraints by warming winters is seen to have had a large influence on natural communities, with resulting high economic and social impact, e.g., the current dramatic mountain pine beetle infestations of western North America (7, 8).

Palms as Indicators of Winter Temperatures

Eocene temperature seasonality has been characterized using proxy thermometers such as palms (Arecaceae), whose seeds and seedlings cannot survive sustained freezing, today limiting their natural distribution to regions of CMMT >5 °C (3, 9), although some palms may tolerate CMMT ∼2.5 °C (Fig. 1). Freezing tolerance is reduced under high atmospheric CO_2, so Eocene records of palms may indicate CMMT >8 °C (10, 11).

Consequently, the overwhelming greatest diversity of genera and species of palms is now restricted to the tropics, with only a few genera occurring outside of it and the subtropics (12). The most cold-tolerant of all living palms, inhabiting the limits of this range, are almost exclusively members of the tribes Trachycarpeae (e.g., *Rhapidophyllum hystrix*, *Serenoa repens, Trachycarpus fortunei*, and *Washingtonia filifera*), Cryosophileae (e.g., *Trithrinax* spp.), and Sabaleae (i.e., *Sabal minor*), all in the subfamily Coryphoideae, with only the New Zealand arecoid palm *Rhopalostylis sapida* matching their cold-tolerance (Fig. 1).

In the Eocene, the range of palms extended into regions of cooler MAT well outside their modern latitudinal limits (3, 11, 13, 14), supporting the reconstruction of globally more equable climates, i.e., milder winters in cooler regions. For example, in the Early Eocene Okanagan Highlands series of montane localities of far-western North America (Fig. 2), the vegetative

Significance

Elevated CO_2 combined with globally warm temperatures in the Eocene make its climate ideal for understanding modern global warming and its biotic consequences. Globally low temperature seasonality—the relationship between winter and mean annual temperatures—has been proposed as key to differential Eocene biodiversity and community patterns. Palms are important winter temperature indicators by their sensitivity to frost; however, their presence in paleocommunities may be masked by taphonomic constraints and identification difficulties. We used fossil obligate palm-feeding beetles to establish the presence of palms in a cool upland in midlatitude western North America. In this way, we provide a more precise characterization of climate during an important interval of the emergence of modern ecosystems.

Author contributions: S.B.A., G.E.M., D.R.G., and R.W.M. designed research; S.B.A. and G.E.M. analyzed the extant and fossil bruchines; D.R.G. and R.W.M. analyzed the extant and fossil palm records; and S.B.A., G.E.M., D.R.G., and R.W.M. wrote the paper.

The authors declare no conflict of interest.

This article is a PNAS Direct Submission.

Data deposition: Fossils are deposited in the collections of Simon Fraser University, The Royal British Columbia Museum, The Stonerose Interpretive Center (Republic, Washington), and Thompson Rivers University.

[1]To whom correspondence should be addressed. E-mail: sba48@sfu.ca.

This article contains supporting information online at www.pnas.org/lookup/suppl/doi:10.1073/pnas.1323269111/-/DCSupplemental.

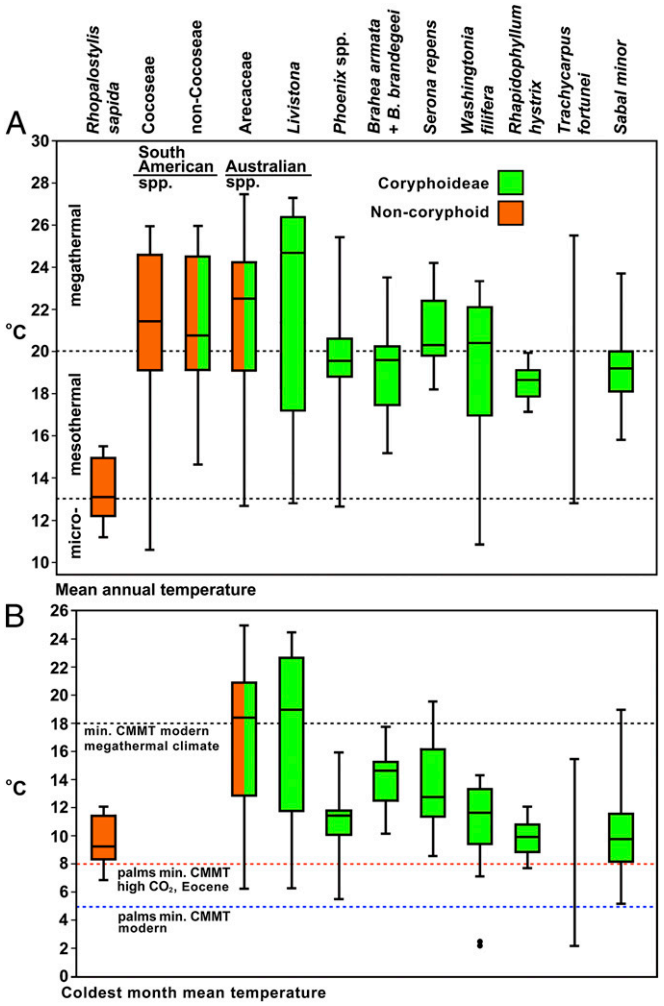

Fig. 1. Climatic profile of palms (median, quartile, and maximum and minimum values), with an emphasis on cold tolerant clades (principally Coryphoids). (*A*) MAT profiles of selected extant palm taxa. (*B*) CMMT profiles of selected extant palm taxa with key thresholds for megathermal (tropical) climates and for palms: CMMT >5 °C for modern palms (with few exceptions: Two outlier occurrences shown as dots are for *W. filifera*) (3); CMMT >8 °C for palms under Eocene levels of atmospheric CO_2 (10). Systematics follows Baker et al. (43).

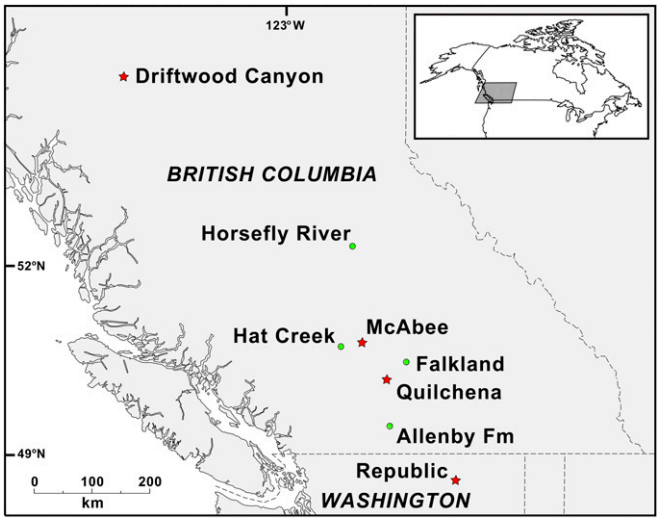

Fig. 2. Map of Early Eocene Okanagan Highland fossil sites. Red stars represent beetle sites: Republic, Quilchena, and McAbee, with confirmed Pachymerina; Republic and McAbee, including beetles assigned to *Caryobruchus* + *Speciomerus*; and Driftwood Canyon with likely Pachymerina. Green dots represent other Okanagan Highlands sites: Allenby Formation with palm macrofossils in chert, *Uhlia allenbyensis* (15); putative palm pollen reported from the Allenby Formation, Quilchena, Falkland, McAbee, Hat Creek, and Driftwood Canyon (for Quilchena, see *Palms as Indicators of Winter Temperatures*; for others, see ref. 18 and references therein). No evidence of palms has been reported from Okanagan Highlands localities at Republic or Horsefly River.

organs of the extinct coryphoid palm *Uhlia allenbyensis* are common in the Princeton Chert (Allenby Formation, BC, Canada), with their anatomy indicating a close affinity to the modern Coryphoideae genera *Brahea, Rhapidophyllum*, and *Serenoa* of the tribe Trachycarpeae (15). Palm macrofossils have not been reported from any of the other Okanagan Highlands Eocene floras (16, 17).

Palm pollen (as *Sabal granopollenites*) has been reported in the Allenby Formation and other Okanagan Highlands sites at Driftwood Canyon, Falkland, Hat Creek, and McAbee (18, 19), although not at others of this series, e.g., Quilchena or Republic. Searches of Quilchena slides prepared by R.W.M. have so far identified only one possible palm pollen grain (Fig. 3) of the *Sabal* type; it is, however, larger (length = 40 μm) than the size range defined by Rouse (20) (28–32 μm) for *S. granopollenites*, and should be referred to *Liliacidites* (21). Harley and Baker (22, 23) reviewed the record of fossil palm-like pollen and express caution in identification, based on its similarity to nonpalm monosulcate monocots and some fossil form genera of nonangiosperm origin. Evidence other than pollen is needed to confirm that palms were distributed widely in the Eocene Okanagan Highlands.

The lack of palm macrofossils from any Okanagan Highlands locality other than the Princeton Chert may reflect that the others are all lacustrine shale localities (except Hat Creek: coal), which might at least in part explain this absence by taphonomic bias. The Chert preserves an in situ aquatic community, and all of the vegetative organs of *U. allenbyensis* are preserved. In lake sediments, however, the persistence of leaves on the trunk after death in many low-statured monocot plants, including coryphoid palms such as most *S. minor*, *S. repens*, and to a limited extent *Trachycarpus* spp., greatly restrict leaf

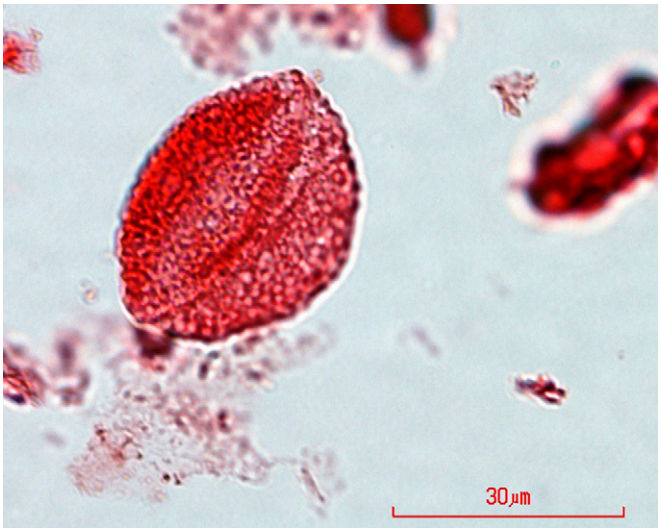

Fig. 3. Fossil palm-like pollen. Early Eocene pollen from the Quilchena (BC, Canada) locality of the Okanagan Highlands resembling palm pollen, but assigned to *Liliacidites*.

fossilization (24). *U. allenbyensis* is reconstructed as a low-statured rhizomatous plant similar in ecology to *S. repens* (15) (Fig. S1). Palms were only recently confirmed at the Florissant locality (Colorado: late Eocene, lacustrine shale) by a single coryphoid palm leaf; long-standing fruit and pollen evidence had been considered controversial (25).

Palm Beetles

Here, we evaluate the Eocene upland winter temperature in the Okanagan Highlands using fossil palm bruchines, beetles of the obligate palm-feeding chrysomelid subtribe Pachymerina as an indicator for the presence of palms where direct macrofossil evidence may be obscured by these factors. In the Eocene, the tribe Pachymerini (bruchines, which includes legume as well as palm feeders) is known from the Early Eocene Okanagan Highlands locality at Quilchena, BC (26), the late Eocene Florissant (27), and an apparently coeval locality in Primorye, Pacific coastal Russia (28); all tentatively assumed to either belong to legume feeding taxa or not associated with host plants. Here, we reexamine the Quilchena beetle and eight new fossils from Okanagan Highlands localities at Driftwood Canyon and McAbee, BC; and Republic, WA (Figs. 2, 4, and 5).

We assign these beetles to the Pachymerini by the following (see terminology in *Materials and Methods*; Figs. S2–S4):

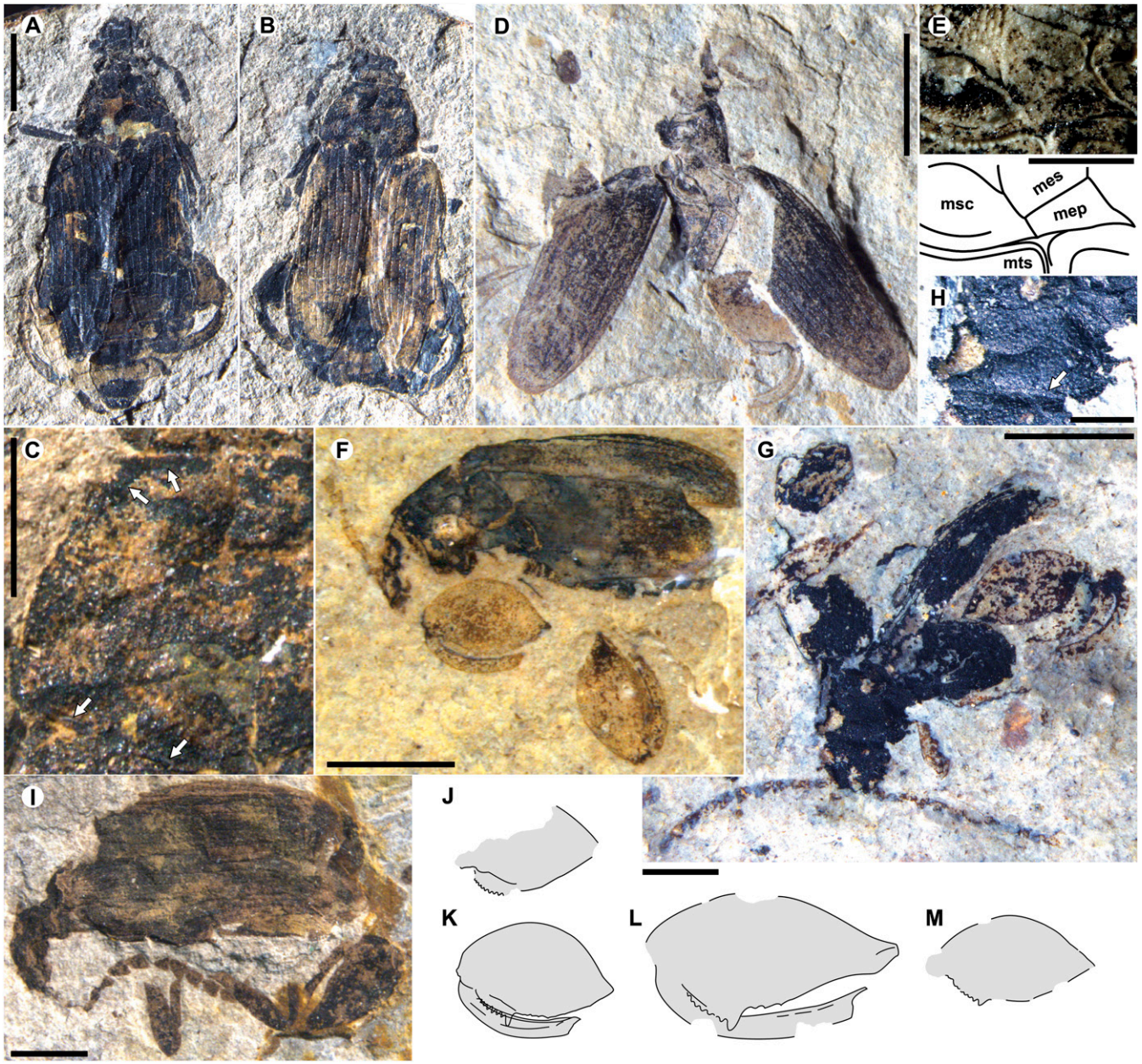

Fig. 4. Quilchena, Republic, and Driftwood Canyon Pachymerina. Specimens from (*A*–*C*) Quilchena, (*D*–*H*, *J*, *K*, and *M*) Republic, and (*I* and *L*) Driftwood Canyon. (*A*) Q-0061a part and (*B*) counterpart. (*C*) Q-0061b, showing impressed marginal line (arrows) surrounding pronotum; (top) anterior margin. (*D*) SR 05-03-10. (*E*) Detail (photograph and drawing) of SR 05-03-10 showing mesepimeron, extending and broad mesally. mep, mesepimeron; mes, mesopleuron; msc, mesocoxal cavity; mts, metasternum. (*F*) SR 99-78-71. (*G*) SRUI 00-94-80, (*H*) Detail showing impressed line on anterior margin (arrow). (*I*) RBCM.EH2013.031.0001.001. (*J*–*M*) Drawings of metafemora of SR 05-03-10, SR 99-78-71, RBCM.EH2013.031.0001.001, and SRUI 00-94-80 respectively. Metatibiae also on *K* and *L*. (Scale bars: 2 mm in *A*, *D*, *F*, *G*, and *I*; *B* is the same scale as in *A*; and 1 mm in *C* and *J*–*M*; 500 μm in *E* and *H*.) (*E*–*G*) Wetted with ethanol.

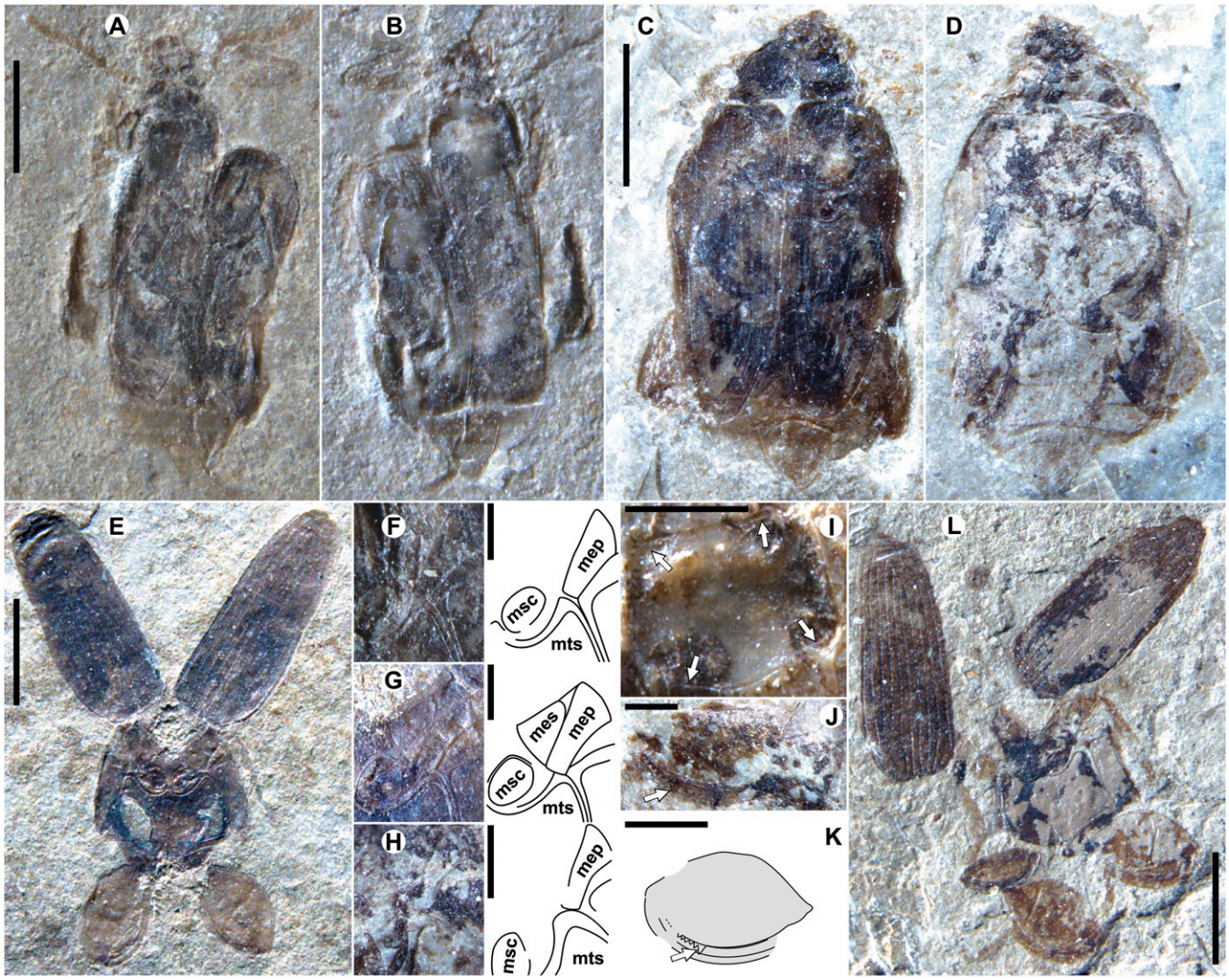

Fig. 5. McAbee Pachymerina. (*A*) F-1542. (*B*) F-1543, counterpart of F-1542. (*C*) F-1540, showing dorsal morphology. (*D*) F-1541, counterpart of F-1540, showing ventral morphology. (*E*) F-939, ventral, pleural portions of the meso- and metathoracic segments, elytra (top) and hind legs (bottom) preserved. (*F–H*) Details (photographs and drawings) showing mesepimeron broad mesally (Fig. 4*E* and abbreviations therein) of F-1542, F-939, and F-1541 respectively. (*I*) F-1543 showing impressed marginal line (arrows) surrounding pronotum; (top) anterior margin. (*J*) Hind leg of F-1541, arrow shows position of denticle 1, *distad* midfemur. (*K*) Drawing of femur and tibia of F-1544, arrow indicating denticle 1; orientation as in *J* (distal femur to the left). (*L*) F-1544, preserved portions mostly as for *E*. (Scale bars: 2 mm in *A*, *C*, *E*, and *L*; *B* is the same scale as *A* and *B*, and *D* as *C*; 1 mm in *I* and *K*; and 500 μm in *F–H* and *J*.)

mesepimeral plate broadly joining the mesocoxa (plesiomorphic for bruchines) combined with metafemora incrassate, with pecten; metatibiae arcuate and mucronate, mucro wedge-shaped; and metacoxa about half-width of metafemur and first sternite (29, 30). We further determined them as palm bruchines, Pachymerina (Table 1 and Figs. 4 and 5), by the presence of either an impressed marginal line extending to the lateral/anterior margins of the pronotum, or broadly triangular tarsomeres one and two on the fore- and midlegs (27, 29, 30).

Results

We found all but one (from Driftwood Canyon) to be palm bruchids, including the Quilchena beetle; its previous tentative association with the Caryopemina (26) was incorrect. In Republic specimens SR 99-94-80 and SRUI 99-78-71 (Fig. 4), and McAbee specimens F-1540/1 and F-1544 (Fig. 5), the pecten positioned *mesad* the metatibia in the flexed hind leg excludes *Pachymerus*, and the pecten placed in the distal portion of the metafemur further excludes *Pachymerus* and also *Caryoborus*, placing these beetles in the *Caryobruchus–Speciomerus* group. *Caryobruchus* and *Speciomerus* are separated by fine details of morphology not preserved in these specimens. Modern species of *Caryobruchus* show a marked preference for palm seeds of the coryphoid tribes Coryphaea, Phoeniceae, and Hyphorbeae, whereas recorded hosts of *Speciomerus* are found within the Arecoid Cocoaceae (31).

Assignment of the single Driftwood Canyon beetle RBCM.EH2013.031.0001.001 (Fig. 4 *I* and *L*) to subtribe level is problematic by preservation, as it bears a damaged and incomplete pronotum and lacks the distal portions of its fore- and middle legs. Its pecten morphology and positioning in the flexed hind leg is, as above, distinctive of *Caryobruchus* and *Speciomerus* when these character states are found within the Pachymerina; however, these are also characteristic of some Old World Caryedontina, a possibility that cannot be excluded here. Within the Caryedontina, *Afroredon* is clearly excluded by its distinctively squat shape; *Exoctenophorus* by the pecten *mesad* the tibia in the flexed hind leg; and *Caryotrypes* by antennal morphology (segments slender, 5–10 feebly serrate in *Caryotrypes*). It is possible that it belongs to the tropical *Mimocaryedon*, which is only known

Table 1. Fossil beetle diagnostic characters, localities, ages, and MAT values

Locality	Specimen	Age, Ma	MAT, °C	MW	MP	IL	TM	PS	PT
Republic		49.4 ± 0.5*	13.5 ± 2.2†						
	SR 99-94-80					X		X	
	SR 05-03-10				X			X	
	SRUI 99-78-71					X		X	X
Quilchena		51.5 ± 0.4‡	14.8 ± 2.0†–15.0 ± 0.6†						
	Q-0061					X	X		
McAbee		52.90 ± 0.83*	9.5§–13.5 ± 2.5†						
	F-1540/1			X	X	X		X	X
	F-1542/3			X				X	X
	F-1544				X	X			
	F-939				X			X	
Driftwood Canyon		51.77 ± 0.34*	6.2 ± 4.7†–12.3 ± 1.9†						
	RBCM.031							X	X

MAT values are from both leaf physiognomy and nearest living relative analyses, which provide the lower and upper values for each site, respectively. MW and MP are diagnostic of Pachymerini (MP within Buchinae); IL and TM of Pachymerina; PS of *Caryobruchus* and *Speciomerus* (within Pachymerina), and PT of *Caryobruchus*, *Speciomerus*, and *Caryoborus* (when these character states are found within Pachymerina) (28, 29). IL, impressed marginal line extending to anterior lateral and anterior margins of the pronotum; MW, metacoxae about half width of metafemorae and first sternite; MP, mesepimeral plate broad mesally, meets mesocoxa and/or metasternum; PS, pecten short, *distad* midfemur; PT, pecten *mesad* tibia on flexed hind leg; RBCM.031, RBCM.EH2013.031.0001.001; TM, broadly triangular tarsomeres 1 and 2 on the fore- and midleg.
*Moss et al. (18).
†Greenwood et al. (16).
‡Villeneuve and Mathewes (46).
§Dillhoff et al. (47).

from Lake Manyara, Tanzania (3.75° S latitude, 955 m elevation) (32), or to the genus *Caryedon*, which today ranges widely through Africa (best known in the tropics), the eastern Mediterranean, Arabian Peninsula, southern Black Sea to Caspian Sea region, and tropical and subtropical South and Southeast Asia (33).

Discussion

These findings provide robust support for the presence of palms at Quilchena and McAbee previously suggested by tentative pollen evidence, and further at Republic, where evidence of palms has not been recovered. The Driftwood Canyon beetle as Pachymerina would provide support for pollen evidence of palms there; but even a Caryedontina affinity would place it in a group with a marked modern preference for tropical to subtropical climates. We also examined beetles from the late Eocene Florissant Formation, confirming their association with the Pachymerina (27), consistent with the recent confirmation of palms there (25). We did not examine the Russian beetle; however, Zherikhin assigned it to the same genus as those from Florissant (28).

All of the Okanagan Highlands localities considered here have estimated microthermal climates (i.e., MAT ≤13 °C) except Quilchena, which is thought to have been lower mesothermal (Table 1).

Peak regional tectonic uplift during Okanagan Highlands times resulted in a mountainous topography comparable to the modern British Columbian Coast and Selkirk ranges (34, 35). Floral proxies indicate a considerably warmer climate in coeval nearby coastal lowland formations, with a substantial elevational MAT gradient upslope to the cooler Okanagan Highlands (16, 17, 19, 36–39). It is highly unlikely that all localities bearing Pachymerina were situated at the precise elevation of the coldest limits of palm tolerance. Any deviation would have to be downslope, i.e., warming winters relative to the established MAT estimates, not cooling them, and Okanagan Highland palms would then have been growing in a climate of even narrower temperature seasonality than is suggested by their minimum winter temperature tolerance.

The climates and communities of numerous hot lowland fossil localities deposited in the EECO have been examined, such as the megathermal Green River Formation in the midcontinental United States (for a review of Green River climates, see refs. 5 and 40). The establishment of warmed winters by the presence of palms in such communities does not, however, indicate reduced temperature seasonality as would their presence in the cooler Okanagan Highlands communities, where they constrain winter temperatures closer to microthermal and lower mesothermal MAT values established independently by bioclimatic and leaf physiognomy analyses (16, 40). Previous analysis based on paleobotanical proxies indicates that McAbee summers were not excessively hot (3). High EECO summer temperatures cannot be excluded, however (e.g., see isotopic analyses for the Bighorn Basin) (41), as the physiological limits of warmer summer temperatures on plants and therefore plant-based proxies, is not well constrained (40). General patterns of Okanagan Highlands summer temperatures would, however, follow from the relationship between CMMT and MAT by definition.

The presence of Pachymerina implies mild winters (Figs. S5 and S6) across this cooler montane setting from northern Washington into midlatitude Canadian localities, all a few degrees more northerly in the Eocene (42). This strengthens the supposition of equable Eocene extratropical climates, with the consequent implications for a globally nonmodern climatic context impacting the emergence of modern ecosystems in the late greenhouse world.

Materials and Methods

We examined nine fossil beetles from four localities of the Okanagan Highlands series of Early Eocene fossil localities: three from Republic, WA, on loan from the Stonerose Interpretive Center (SR 05-03-10; SR99-78-71a, b; SRUI 00-94-80); one from Quilchena, BC, in the Simon Fraser University collection (Q-0061a, b); four from McAbee, BC, on loan from Thompson Rivers University (UCCIPR L-18 F-1540/1; F-1542/3; and F-1544); and one from Driftwood Canyon, BC, on loan from BC Parks (RBCM.EH2013.031.0001.001). We follow the palm systematics of Baker et al. (43) and the beetle systematics of Nilsson and Johnson (30). Subtribe Pachymerina (palm bruchines) was previously considered by many authors as the tribe Pachymerini *sensu* Nilsson and Johnson (30), with Bruchinae the family Bruchidae; we treat the Bruchinae as a subfamily of the Chrysomelidae and adjust references to previously published ranks accordingly.

Analyses. Climate range analyses for both the beetles (Tables S1–S4) and palms (Fig. 1) used existing data sources (references in *SI Text*) or were done using the DIVA-GIS software (www.diva-gis.org) with the WorldClim dataset

(www.worldclim.org) to generate estimates of MAT, winter temperature [coldest quarter mean temperature ~1–2 °C warmer than CMMT, which palm climate ranges are reported in] and mean annual precipitation for modern localities to a 1-km square resolution (44). Climate analyses for palms further used ANUCLIM 6.1 (45) for the Australian records.

Terminology (Figs. S2–S4).

Metafemora incrassate: femora of the hind leg thickened, swollen.

Pecten: comb-like structure on the posterior–ventral portion of metafemora.

Denticles: projections from pecten forming "teeth of the comb."

Metatibia arcuate: tibia of the hind leg curved.

Metatibia mucronate: projection (mucro) extending from distal surface of the hind tibiae.

Metatibia carinate: with grooves (carinae) running lengthwise along the hind tibiae.

Mesocoxa: basal segment of the middle leg, attaching the leg to the thorax.

Metacoxa: basal segment of the hind leg.

Tarsomeres: subdivisions of the tarsus, portion of the leg *distad* the tibia.

Mesepimeron: posterior division of the middle thoracic pleuron (exterior, side).

Impressed marginal line on pronotum: a groove on the dorsal surface of the pronotum, just inside its margin.

ACKNOWLEDGMENTS. We thank BC Parks and J. Howard (BC Parks, Smithers) for facilitating fieldwork at the Driftwood Canyon Provincial Park; G. Rose for facilitating fieldwork at Quilchena; G. Wilson, G. Bacon, and K. Volkman for the donation of Republic specimens (to Stonerose Interpretive Center) and C. Brown for their loan; D. Langevin for the donation of one of the McAbee specimens [to Thompson Rivers University (TRU)] and N. Van Wagoner for TRU specimen loans; D. Langevin, R. Campbell, and R. Drachuck for facilitating fieldwork at McAbee; C. Labandeira, D. Levin, and F. Marsh (Smithsonian Institution) and B. Farrell and P. Perkins (Museum of Comparative Zoology) for Florissant specimen loans; V. Makarkin for Russian papers and translations; and M. Pellatt (Parks Canada) for the use of digital microphotography equipment. This work was funded by a Natural Sciences and Engineering Research Council (NSERC Canada) fellowship (to S.B.A.) and NSERC Discovery Grants 311934 (to D.R.G.) and 3835 (to R.W.M.). We thank an anonymous donor for travel funding and imaging equipment in San Diego.

1. Zachos JC, Dickens GR, Zeebe RE (2008) An early Cenozoic perspective on greenhouse warming and carbon-cycle dynamics. *Nature* 451(7176):279–283.
2. Secord R, et al. (2012) Evolution of the earliest horses driven by climate change in the Paleocene-Eocene Thermal Maximum. *Science* 335(6071):959–962.
3. Greenwood DR, Wing SL (1995) Eocene continental climates and latitudinal temperature gradients. *Geology* 23(11):1044–1048.
4. Archibald SB, Bossert WH, Greenwood DR, Farrell BD (2010) Seasonality, the latitudinal gradient of diversity, and Eocene insects. *Paleobiology* 36(3):374–398.
5. Archibald SB, Johnson KR, Mathewes RW, Greenwood DR (2011) Intercontinental dispersal of giant thermophilic ants across the Arctic during early Eocene hyperthermals. *Proc Biol Sci* 278(1725):3679–3686.
6. Archibald SB, Greenwood DR, Mathewes RW (2013) Seasonality, montane beta diversity, and Eocene insects: Testing Janzen's dispersal hypothesis in an equable world. *Palaeogeogr Palaeoclimatol Palaeoecol* 371:1–8.
7. Powell JA, Logan JA (2005) Insect seasonality: Circle map analysis of temperature-driven life cycles. *Theor Popul Biol* 67(3):161–179.
8. Raffa KF, Powell EN, Townsend PA (2013) Temperature-driven range expansion of an irruptive insect heightened by weakly coevolved plant defenses. *Proc Natl Acad Sci USA* 110(6):2193–2198.
9. Larcher W, Winter A (1981) Frost susceptibility of palms: Experimental data and their interpretation. *Principes* 25:143–152.
10. Royer DL, Osborne CP, Beerling D (2002) High CO2 increases the freezing sensitivity of plants: Implications for paleoclimatic reconstructions from fossil floras. *Geology* 30(11):963–966.
11. Sluijs A, et al. (2009) Warm and wet conditions in the Arctic region during Eocene Thermal Maximum 2. *Nat Geosci* 2(11):777–780.
12. Eiserhardt WL, Svenning J-C, Kissling WD, Balslev H (2011) Increased seasonality through the Eocene to Oligocene transition in northern high latitudes. *Ann Bot (Lond)* 108:1391–1416.
13. Eldrett JS, Greenwood DR, Harding IC, Huber M (2009) Increased seasonality through the Eocene to Oligocene transition in northern high latitudes. *Nature* 459(7249):969–973.
14. Pross J, et al.; Integrated Ocean Drilling Program Expedition 318 Scientists (2012) Persistent near-tropical warmth on the Antarctic continent during the early Eocene epoch. *Nature* 488(7409):73–77.
15. Erwin DW, Stockey RA (1991) Silicified monocotyledons from the Middle Eocene Princeton chert (Allenby Formation) of British Columbia, Canada. *Rev Palaeobot Palynol* 70:147–162.
16. Greenwood DR, Archibald SB, Mathewes RW, Moss PT (2005) Fossil biotas from the Okanagan Highlands, southern British Columbia and northern Washington State: Climates and ecosystems across an Eocene landscape. *Can J Earth Sci* 42(2):167–185.
17. Smith RY, Basinger JF, Greenwood DR (2012) Early Eocene plant diversity and dynamics in the Falkland flora, Okanagan Highlands, British Columbia, Canada. *Palaeobiodivers Palaeoenviron* 92:309–328.
18. Moss PT, Greenwood DR, Archibald SB (2005) Regional and local vegetation community dynamics of the Eocene Okanagan Highlands (British Columbia – Washington State) from palynology. *Can J Earth Sci* 42(2):187–204.
19. Dillhoff RM, Dillhoff TA, Greenwood DR, DeVore ML, Pigg KB (2013) The Eocene Thomas Ranch flora, Allenby Formation, Princeton, British Columbia, Canada. *Botany* 91(8):514–529.
20. Rouse GE (1962) Plant microfossils from the Burrard Formation of western British Columbia. *Micropaleontology* 8(2):187–218.
21. Nichols J, Ames HT, Traverse A (1973) On *Arecipites* Wodehouse, *Monocolpopollenites* Thomson & Pflug, and the species "*Monocolpopollenites tranquillus*". *Taxon* 22(2-3): 241–256.
22. Harley MM, Baker WJ (2001) Pollen aperture morphology in Arecaceae: Application within phylogenetic analyses, and a summary of record of palm-like pollen the fossil. *Grana* 40(1-2):45–77.
23. Harley MM (2006) A summary of fossil records for Arecaceae. *Bot J Linn Soc* 151(1):39–67.
24. Smith SY (2013) The fossil record of non-commelinid monocots. *Early Events in Monocot Evolution*, eds Wilkin P, Mayo SJ (Cambridge Univ Press, Cambridge, UK), Systematics Association Special Vol 83, pp 29–59.
25. Manchester SR (2001) Update on the Megafossil flora of Florissant, Colorado. *Fossil Flora and Stratigraphy of the Florissant Formation, Colorado*. Proceedings of the Denver Museum of Nature and Science, eds Evanoff E, Gregory-Wodzicki K, Johnson K. Series 4, No 1, pp 137–161.
26. Archibald SB, Mathewes RW (2000) Early Eocene insects from Quilchena, British Columbia and their paleoclimatic implications. *Can J Zool* 78(8):1441–1462.
27. Kingsolver JM (1965) A new fossil bruchid genus and its relationship to modern genera (Coleoptera: Bruchidae: Pachymerinae). *Col Bull* 19(1):25–30.
28. Zherikhin VV (1989) *Kainozoi Dal'nego Vostoka*, eds Krasilov VA, Klimova RS (Far Eastern Branch of Academy of Sciences of the USSR, Vladivostok, Russia), pp 1–250.
29. Bridwell JC (1929) A preliminary generic arrangement of the palm bruchids and allies (Coleoptera) with descriptions of new species. *Proc Entomol Soc Wash* 31(8):141–160.
30. Nilsson JA, Johnson CD (1993) A taxonomic revision of the palm bruchids (Pachymerini) and a description of the world genera of Pachymerinae (Coleoptera: Bruchidae). *Mem Am Entomol Soc* 41:1–104.
31. Johnson CD, Zona S, Nilsson JA (1995) Bruchid beetles and palm seeds: Recorded relationships. *Principes* 39(1):25–35.
32. Decelle J (1968) Nouveaux genres et especes de Caryedontini (Col. Bruchidae, Pachymerinae) d'Afrique et de Madagascar. *Bull Ann Soc R Entomol Belg Entomol* 104: 413–426.
33. Borowiec L (1987) The genera of seed-beetles (Coleoptera Bruchidae). *Pol Pismo Entomol* 57:3–206.
34. Ewing TE (1980) Paleogene tectonic evolution of the Pacific Northwest. *J Geol* 88(6): 619–638.
35. Tribe S (2005) Eocene paleo-physiography and drainage directions, southern Interior Plateau, British Columbia. *Can J Earth Sci* 42(2):215–230.
36. Smith RY, Basinger JF, Greenwood DR (2009) Depositional setting, floristics and paleoenvironment of the Early Eocene Falkland site, a new fossil flora locality from the Okanagan Highlands, British Columbia. *Can J Earth Sci* 46(11):811–822.
37. Rouse GE, Hopkins WS, Jr., Piel KM (1971) Palynology of some Late Cretaceous and Early Tertiary deposits in British Columbia and adjacent Alberta. *Symposium on Palynology of the Late Cretaceous and Early Tertiary*, eds Kosanke RM, Cross AT. *Geol S Am S* 127:213–246.
38. Mustoe GE, Gannaway WL (1997) Paleogeography and paleontology of the Early Tertiary Chuckanut Formation, Northwest Washington. *Wash Geol* 25(3):3–18.
39. Wolfe JA, Forest CE, Molnar P (1998) Paleobotanical evidence of Eocene and Oligocene paleoaltitudes in midlatitude western North America. *Geol Soc Am Bull* 110(5): 664–678.
40. Huber M, Caballero R (2011) The early Eocene equable climate problem revisited. *Clim Past* 7:603–633.
41. Snell KE, et al. (2013) Hot summers in the Bighorn Basin during the early Paleogene. *Geology* 41(1):55–58.
42. Andrews JA (1985) True polar wander: An analysis of Cenozoic and Mesozoic paleomagnetic poles. *J Geophys Res* 90(B9):7737–7750.
43. Baker WJ, et al. (2009) Complete generic-level phylogenetic analyses of palms (Arecaceae) with comparisons of supertree and supermatrix approaches. *Syst Biol* 58(2): 240–256.
44. Hijmans RJ, et al. (2005) Very high resolution interpolated climate surfaces for global land areas. *Int J Climatol* 25(15):1965–1978.
45. Xu T, Hutchinson M (2013) New developments and applications in the ANUCLIM spatial climatic and bioclimatic modelling package. *Environ Model Softw* 40:267–279.
46. Villeneuve M, Mathewes R (2005) *An Early Eocene Age for the Quilchena Fossil Locality, Southern British Columbia* (Geol Sur Can Curr Res, Ottawa), 2005-A4, pp 1–7.
47. Dillhoff RM, Leopold EB, Manchester SR (2005) The McAbee flora of British Columbia and its relation to the Early-Middle Eocene Okanagan Highlands flora of the Pacific Northwest. *Can J Earth Sci* 42(2):155–166.

Supporting Information

Archibald et al. 10.1073/pnas.1323269111

SI Text

Data from Collections

California Academy of Sciences collections (CAS)
Arizona State University, Tempe collections (ASUT)
J. Romero Nápoles collections
G. E. Morse collections

Global Biodiversity Information Facility Data

Occurrence data accessed through the Global Biodiversity Information Facility (GBIF) data portal for the following taxa, published online at www.gbif.org by the institutions listed here below (all accessed December 19, 2012):

***Speciomerus giganteus*.**

Coleopteran specimens of Iwate Prefectural Museum
Texas A&M University Insect Collection
Especímenes INBio

***Pachymerus* Species.**

Snow Entomological Museum Collection
Peabody Entomology Distributed Generic Information Retrieval Service
National Museum of Natural History (NMNH) Entomology Collections
Royal Belgian Institute of Natural Sciences collections
Texas A&M University Insect Collection
Illinois Natural History Survey

***Caryobruchus marieae*.**

Texas A&M University Insect Collection

***Caryobruchus gleditsiae*.**

Texas A&M University Insect Collection
Lund Museum of Zoology–Insect collections

Occurrence data accessed through the GBIF data portal for the following taxa, published online there by the institutions listed (accessed April 17–August 18, 2013):

Brahea armata (synonym *Brahea elegans*) and *Brahea brandegeei*:

Missouri Botanical Garden
Herbario de la Universidad de Arizona
Herbario del Centro de Investigaciones Biológicas del Noroeste (HCIB)
Riqueza y distribución de especies
El complejo Brahea–Erythea (Palmae)
NMNH Botany Collections
University of Arizona (UA) Herbarium
Actualización de la base de datos del Herbario de la Universidad de Sonora (USON)
Nationaal Herbarium Nederland
Fairchild Tropical Botanic Garden

Phoenix abyssinica, Phoenix acaulis, Phoenix andamanensis, Phoenix caespitose, Phoenix canariensis, Phoenix dactylifera, Phoenix humilis, Phoenix loureiroi, Phoenix paludosa, Phoenix reclinata, Phoenix roebelenii, and *Phoenix theophrasti*:

Nationaal Herbarium Nederland
Wildlife Institute of India Herbarium Dataset
Royal Botanic Gardens, Kew
Database of the Botany Collection of the Museum of Evolution in Uppsala (UPS)
Universidad de Barcelona. Grup d'Investigació Geobotánica i Cartografía de vegetación a escala de
Universidad de Málaga: MGC-Cormof
Fundación Biodiversidad, Real Jardín
Jardín Botánico de Córdoba: Herbarium
Real Jardin Botanico (Madrid), Vascular
Tercer Inventario Forestal Nacional
Israel Nature and Parks Authority
Generalitat Valenciana. Banco de Datos
Herbario del Jardín Botánico–Histórico
Sistema de Información de la vegetación
Hortus Botanicus Sollerensis Herbarium
The Aarhus University Herbarium Database (AUU)
Missouri Botanical Garden
Herbario de la Universidad de Almeria
Royal Botanic Garden Edinburgh Herbarium (E)
Lund Botanical Museum (LD)

Washingtonia filifera:

US Department of Agriculture (USDA) PLANTS Database, USDA Natural Resources Conservation Service
iNaturalist research-grade observations
CAS Botany (CAS-BOT)
Consortium of California Herbaria
UA Herbarium

Occurrence data accessed through Australia's Virtual Herbarium (1) online, and analyzed using the ANUCLIM 6.1 climate surface software (2) for the following taxa (accessed April 14–20, 2013):

Livistona spp.
Arecaceae (all Australian genera combined, including *Livistona*)

Additional climate range data were accessed from Thompson et al. (3) for these palm taxa:

Rhapidophyllum hystrix
Sabal minor
Serenoa repens

Climate range data for *Rhopalostylis sapida* is from Reichgelt et al. (4), and for *Trachycarpus fortunei* the range data (minimum and maximum only) was from Walther et al. (5). South American Coccoseae and non-Coccoseae palm climate range data from Kissling et al. (6).

1. Council of Heads of Australasian Herbaria (2013) Australia's Virtual Herbarium. Available at http://avh.chah.org.au. Accessed April 20, 2013.
2. Xu T, Hutchinson M (2013) New developments and applications in the ANUCLIM spatial climatic and bioclimatic modelling package. *Environ Model Softw* 40:267–279.
3. Thompson RS, et al. (2012) *Atlas of Relations Between Climatic Parameters and Distributions of Important Trees and Shrubs in North America – Modern Data for Climatic Estimation from Vegetation Inventories* (US Geol Surv, Denver), US Geol Surv Prof Pap 1650–F.

4. Reichgelt T, et al. (2013) Quantitative palaeoclimate estimates for Early Miocene southern New Zealand: Evidence from Foulden Maar. *Palaeogeogr Palaeoclimatol Palaeoecol* 378:36–44.
5. Walther G-R, et al. (2007) Palms tracking climate change. *Glob Ecol Biogeogr* 16(6): 801–809.
6. Kissling WD, et al. (2012) Cenozoic imprints on the phylogenetic structure of palm species assemblages worldwide. *Proc Natl Acad Sci USA* 109(19):7379–7384.

Fig. S1. Modern low-statured aquatic palms. *S. repens*, Florida (*Left* and *Right*); a low-statured palm closely related to the Eocene palm *Uhlia allenbyensis* in an aquatic setting as modeled for the Princeton Chert (Okanagan Highlands, BC, Canada) by Erwin and Stockey (1).

1. Erwin DW, Stockey RA (1991) Silicified monocotyledons from the Middle Eocene Princeton chert (Allenby Formation) of British Columbia, Canada. *Rev Palaeobot Palynol* 70:147–162.

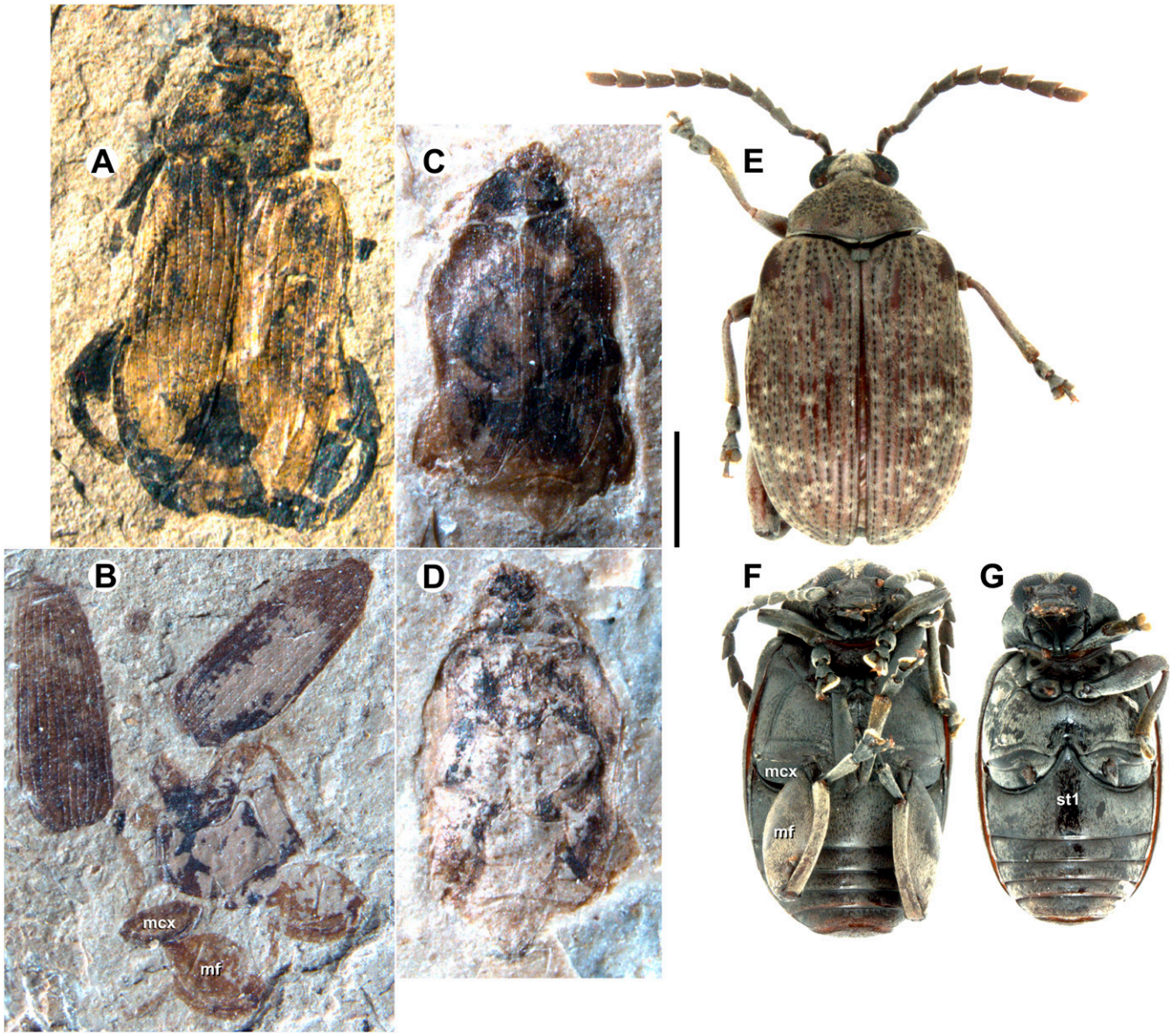

Fig. S2. Fossil and modern Pachymerina dorsal and ventral aspects. Fossil Pachymerina from Quilchena [(*A*) Q-0061, dorsal aspect] and McAbee [(*B*) F-1543, ventral aspect]. (*C*) F-1540 (dorsal) and (*D*) F-1541 [(counterpart of F-1540, same insect), ventral aspects]; and modern Pachymerina, *C. gleditsiae*: (*E*) dorsal, (*F*) ventral, and (*G*) ventral (legs and antennae removed) aspects. Note pecten *mesad* tibia in the flexed hind legs in *F*, a condition found in *Caryobruchus* and *Speciomerus* species. The metacoxae (mcx) are less than half the width of the metafemora (mf) and sternite 1 (st1), which is diagnostic of Pachymerini (*B*, *D*, *F*, and *G*). Metafemorae in *F* are depicted at an oblique angle. Pecten on fossils may often be seen through overlaying tibia as an artifact of preservation; ventral anatomy in general is sometimes visible, impressed through a mostly dorsal aspect fossil (e.g., Fig. 5 *A* and *F*). (Scale bar: 2 mm, all to scale.)

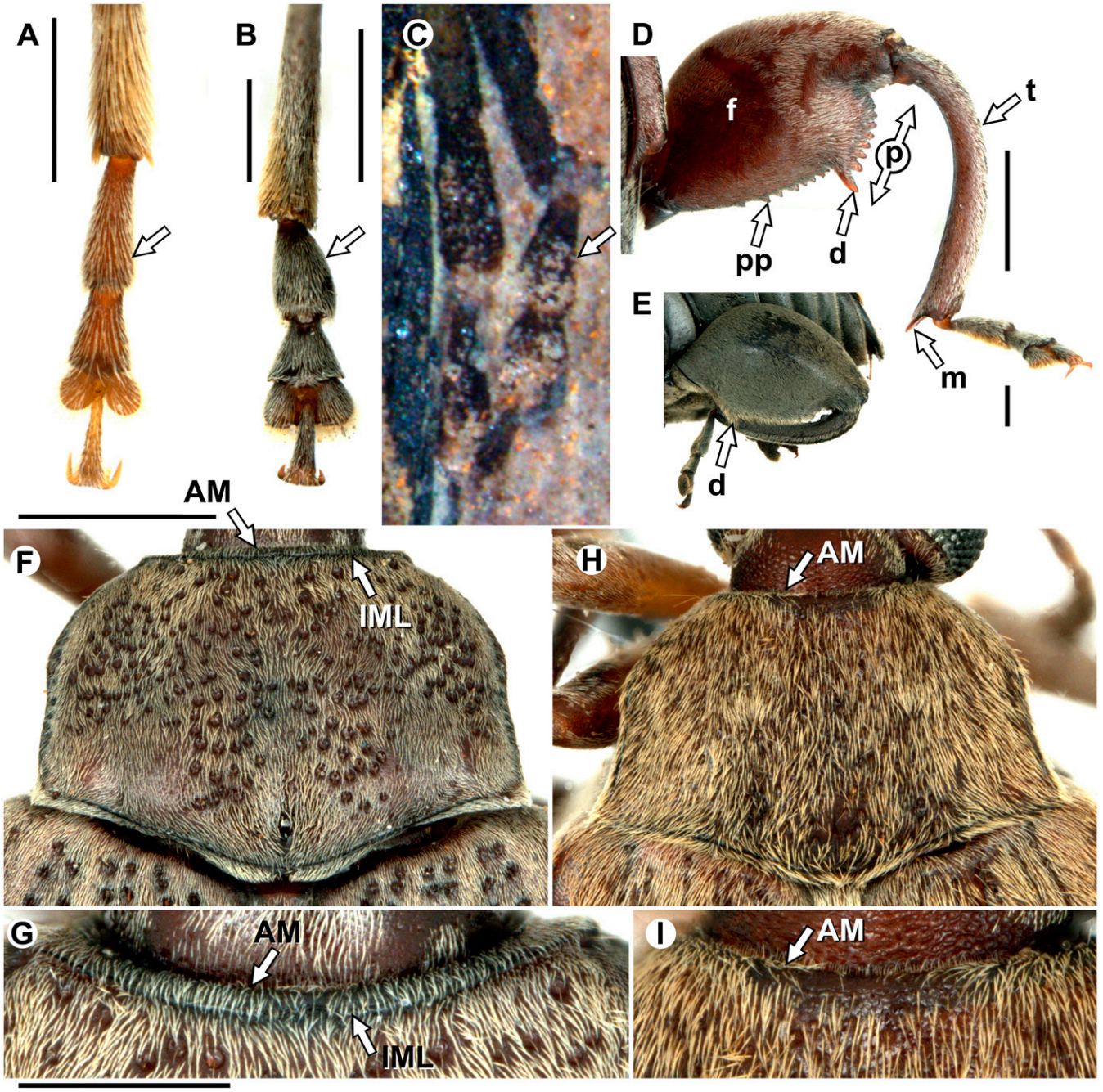

Fig. S3. Characters of the leg and pronotum of Pachymerina. (*A*–*C*) Mesotarsus of (*A*) *Caryedon serratus* (Pachymerini: Caryedontina), with elongate, narrow tarsomere 1 (arrow); and (*B*) *C. gleditsiae* (Pachymerini: Pachymerina), with short, broadly triangular tarsomere 1 (arrow), diagnostic of Pachymerina (fore- and midlegs). (*C*) Tarsus of fore- or midleg of Quilchena Q-0061, with morphology as in *B*. (*D*) Hind leg of *C. gleditsiae*. d, denticle 1 (basal-most part of pecten); f, metafemur; m, mucro; p, pecten; pp, prepectenal ridges; t, metatibia. (*E*) Hind leg of *Pachymerus cardo* showing pecten positioned *laterad* (outside of) metafemur when leg flexed. Note that pecten extends *basad* midfemur. d, denticle 1. (*F*–*I*) Dorsal aspect of pronotum of (*F*) *C. gleditsiae* (Pachymerina) showing and impressed marginal line (IML) along the anterior margin (AM), diagnostic of Pachymerina. (*G*) Close-up of the specimen in (*F*). (*H*) Pronotum of *C. serratus* (Caryedontina) lacking the IML on the AM. (*I*) Close-up of the specimen in *G*. (Scale bars: 1 mm in *A*–*F* and *H* and 500 μm in *G* and *I*.)

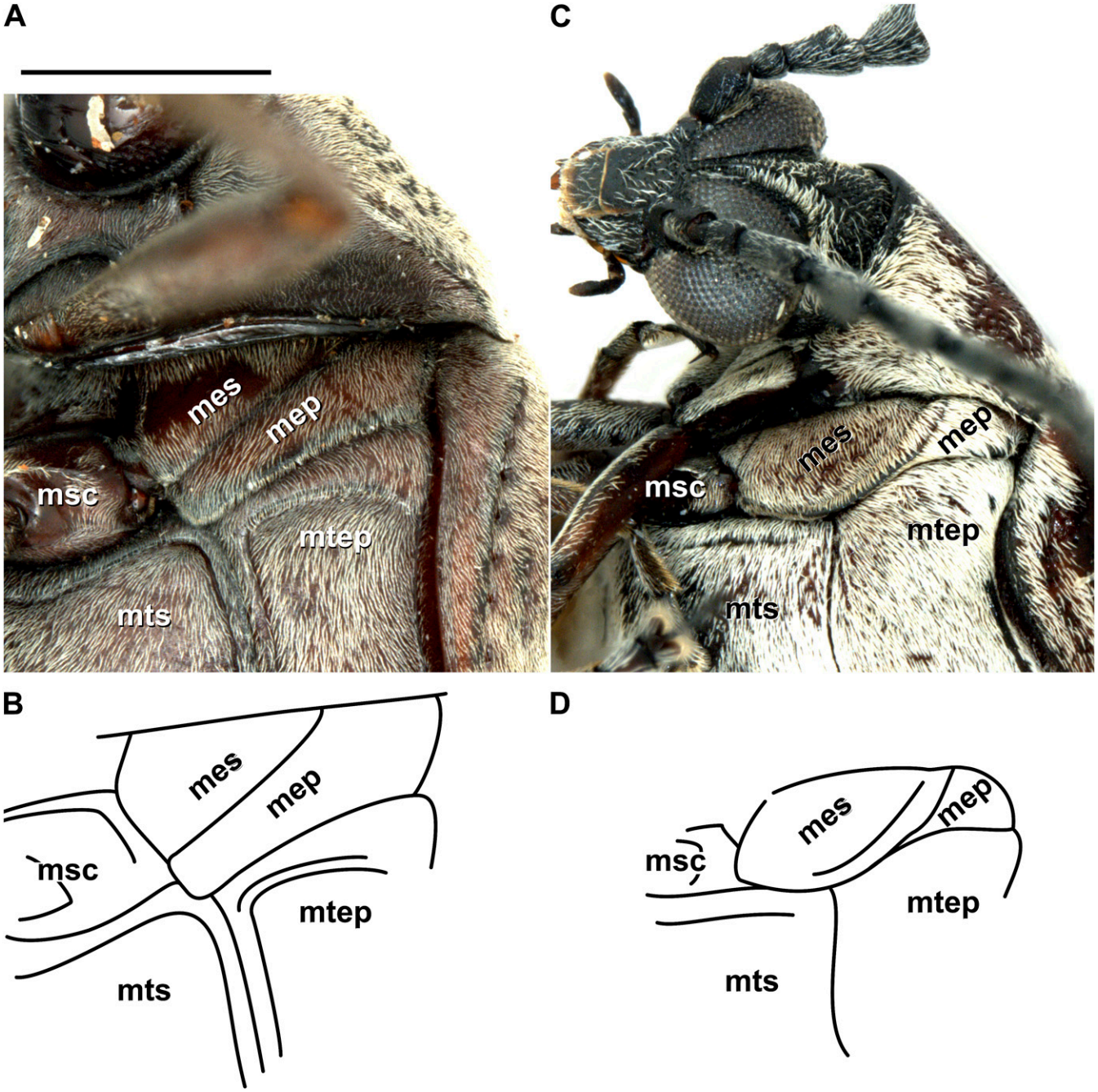

Fig. S4. Pachymerini mesepimeral morphology. Ventrolateral portion of thorax of *C. gleditsiae* (Bruchinae: Pachymerini: Pachymerina) [(*A*) photograph and (*B*) drawing] and *Megacerus discoidus* (Bruchinae: Bruchini: Megacerina) [(*C*) photograph and (*D*) drawing], showing difference in the size, shape, and location of the mesepimeron and mesopleuron. mep, mesepimeron; mes, mesopleuron; msc, mesocoxal cavity; mtep, metepisternum; mts, metasternum. *C. gleditsiae* shows the plesiomorphic condition of the mesepimeron expanded mesally, connecting broadly with the mesocoxa and/or metasternum, contrasted with the derived state seen in *M. discoidus*, where the mesepimeron narrows and may not reach the mesocoxa and/or metasternum. This mesally expanded mesepimeron is not itself diagnostic of Pachymerini or Pachymerina; it appears in other tribes of Bruchinae (Amblycerini, Eubaptini, and Rhaebini); however, this is only found in the Pachymerini in combination with the incrassate metafemur and metatibia carinate (the incrassate metafemur and metatibia carinate without the mesally expanded mesepimeron occurs convergently in a lineage of Bruchini). (Scale bar: 1 mm, all to scale.)

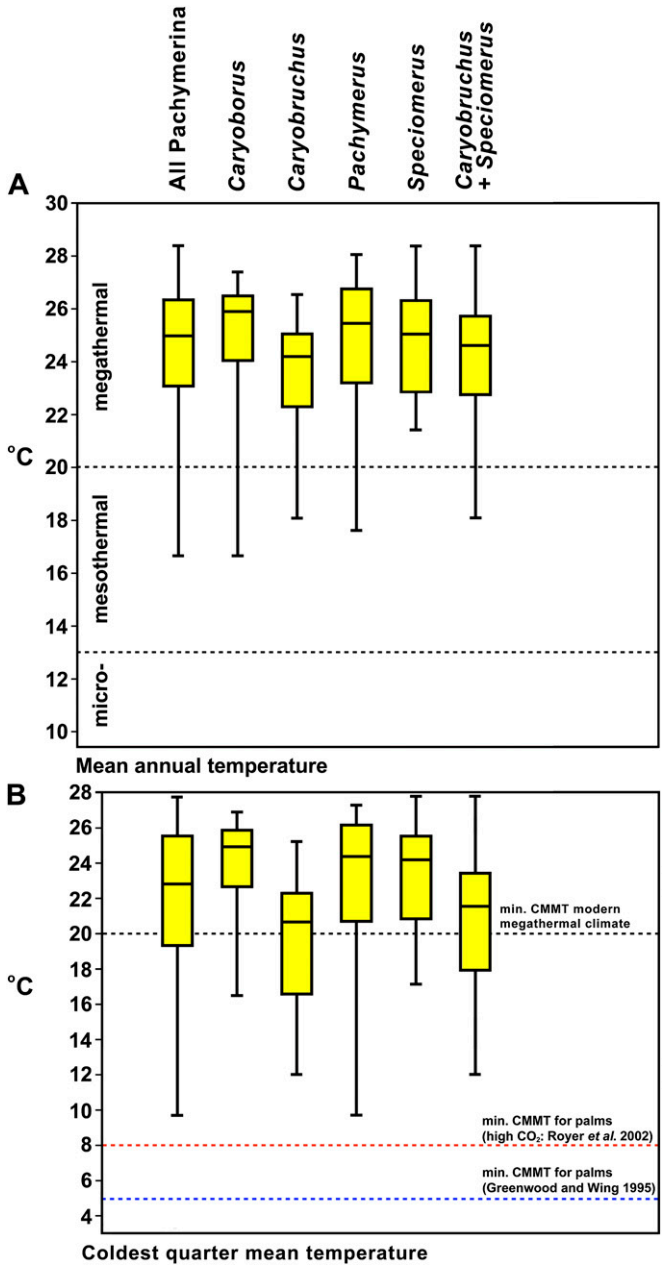

Fig. S5. Climatic profiles for modern Pachymerina; median, quartiles, and maximum and minimum values plotted for each. (*A*) Mean annual temperature (MAT) and (*B*) coldest quarter mean temperature (CQMT) for Pachymerina [CQMT is ~1–2 °C warmer than the coldest month mean temperature (CMMT)]. Fossils reported here are from microthermal to lower mesothermal climates. *B* shows the minimum CMMT for modern megathermal climates (black dashed line); the range of some Pachymerina extends outside of megathermal climates (the tropics) (Fig. S6). The blue dashed line is the minimum modern CMMT for palms (1), with very few exceptions (Fig. 1). The red dashed line shows the minimum CMMT as modeled for the high CO_2 conditions of the Eocene (2, 3). Fossils are assigned to Pachymerina (Republic, McAbee, and Quilchena) and some to *Caryobruchus* + *Speciomerus* (Republic and McAbee), or likely Pachymerina and if so, *Caryobruchus* + *Speciomerus* (Driftwood Canyon). Data from Table S4.

1. Greenwood DR, Wing SL (1995) Eocene continental climates and latitudinal temperature gradients. *Geology* 23(11):1044–1048.
2. Royer DL, Osborne CP, Beerling D (2002) High CO2 increases the freezing sensitivity of plants: Implications for paleoclimatic reconstructions from fossil floras. *Geology* 30(11):963–966.
3. Sluijs A, et al. (2009) Warm and wet conditions in the Arctic region during Eocene Thermal Maximum 2. *Nat Geosci* 2(11):777–780.

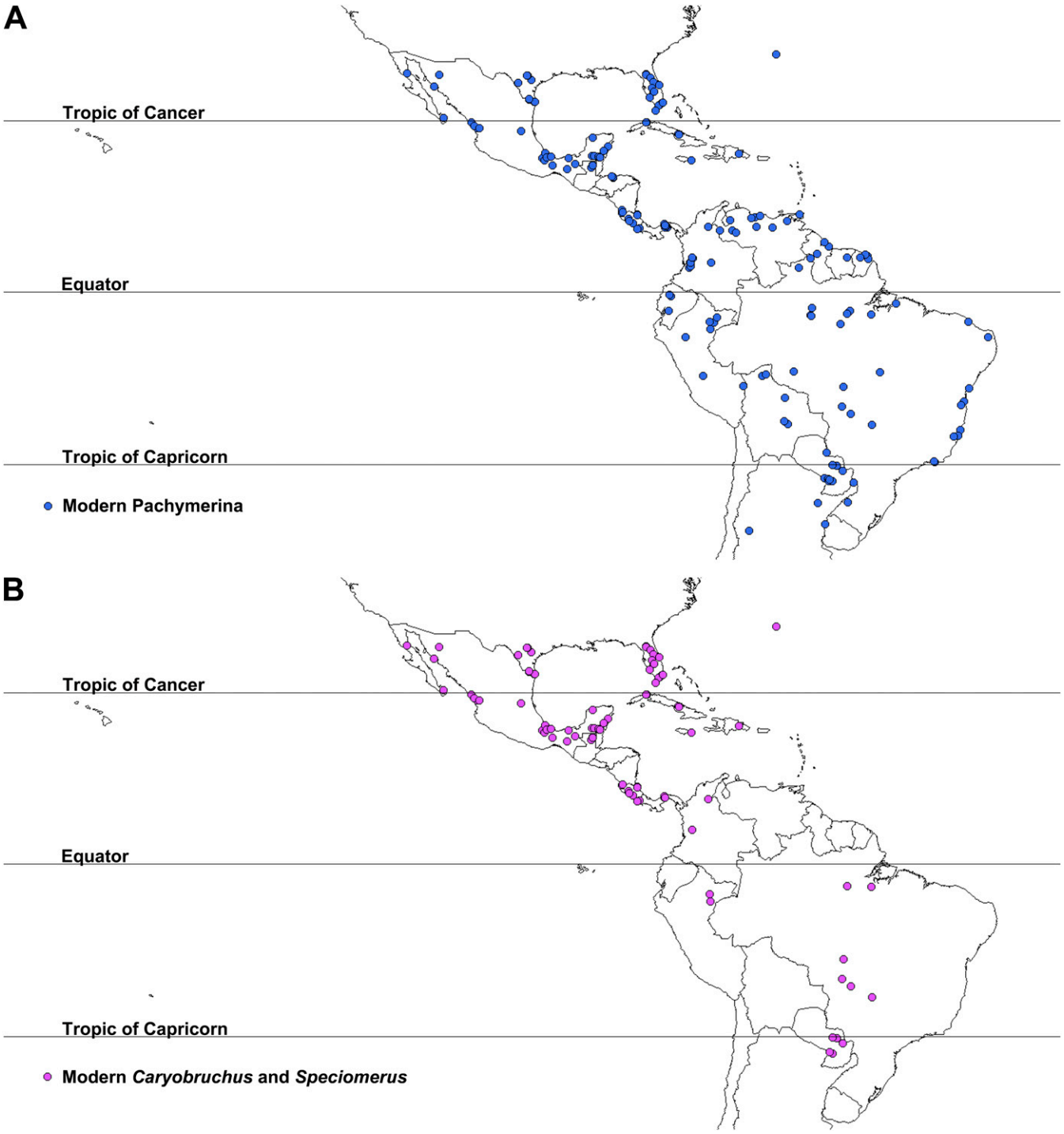

Fig. S6. Maps of modern Pachymerina occurrences. (*A*) modern occurrences of Pachymerina, and (*B*), modern occurrences of *Caryobruchus* + *Speciomerus* species: Both are data from Table S4.

Table S1. Pachymerina occurrence MATs

Group	Minimum	25th	Median	75th	Maximum
All Pachymerina	16.74	23.13	25.04	26.39	28.43
Caryoborus	16.74	24.10	25.96	26.54	27.45
Caryobruchus	18.16	22.36	24.25	25.11	26.60
Pachymerus	17.69	23.26	25.51	26.80	28.10
Speciomerus	21.48	22.91	25.10	26.37	28.43
Caryobruchus + *Speciomerus*	18.16	22.81	24.67	25.78	28.43

MAT values in °C. Data from Table S4.

Table S2. Pachymerina occurrence winter temperatures

Group	Minimum	25th	Median	75th	Maximum
All Pachymerina	9.70	19.40	22.90	25.65	27.87
Caryoborus	16.52	22.72	25.00	25.94	26.98
Caryobruchus	12.02	16.60	20.72	22.35	25.30
Pachymerus	9.70	20.74	24.45	26.24	27.37
Speciomerus	17.17	20.88	24.24	25.60	27.87
Caryobruchus + *Speciomerus*	12.02	17.95	21.60	23.48	27.87

CQMT values in °C. Data from Table S4.

Table S3. Pachymerina occurrence mean annual precipitation

Group	Minimum	25th	Median	75th	Maximum
All Pachymerina	115	1,258	1,538	2,285	5,033
Caryoborus	539	1,612	2,327	2,711	3,766
Caryobruchus	115	941	1,275	1,437	2,777
Pachymerus	150	1,267	1,717	2,168	2,855
Speciomerus	1,348	1,535	1,915	2,690	5,033
Caryobruchus + *Speciomerus*	115	1,238	1,411	1,874	5,033

Mean annual precipitation (MAP) values in millimeters per year. Data from Table S4.

Table S4. Pachymerina occurrence and climate data used in Tables S1–S3

Species	Country	Latitude	Longitude	MAT	CQMT	MAP	Source
Caryoborus chiriquensis	Ecuador	−0.4356	−78.9656	16.74	16.52	2,341	1
Caryoborus chiriquensis	Ecuador	−0.2542	−79.1725	23.13	22.53	2,706	1
Caryoborus chiriquensis	Honduras	15.5333	−86.8000	18.93	16.62	1,650	2
Caryoborus chiriquensis	Panama	9.3494	−79.9044	26.74	26.10	3,256	3
Caryoborus gracilis	Bolivia	−11.3175	−66.5789	26.30	25.00	1,599	1
Caryoborus gracilis	Bolivia	−17.8000	−63.1667	23.95	20.63	1,244	1
Caryoborus gracilis	Brazil	4.7167	−60.0167	23.78	23.40	1,261	1
Caryoborus gracilis	Brazil	−10.6667	−62.3000	24.20	23.57	1,923	1
Caryoborus gracilis	Colombia	4.1014	−73.5647	25.85	25.00	3,568	1
Caryoborus gracilis	Ecuador	−0.2542	−79.1725	23.13	22.53	2,706	1
Caryoborus gracilis	French Guiana	4.8167	−53.2667	25.23	24.63	2,664	1
Caryoborus gracilis	Peru	−11.2542	−74.6367	23.53	22.67	1,754	1
Caryoborus gracilis	Peru	−4.9081	−73.6667	26.83	26.25	2,632	4
Caryoborus gracilis	Peru	−3.9167	−73.7500	26.39	25.80	2,712	4
Caryoborus gracilis	Peru	−3.4000	−72.7500	26.23	25.58	2,873	4
Caryoborus gracilis	Peru	−4.9167	−73.6667	26.83	26.25	2,632	4
Caryoborus gracilis	Venezuela	9.7500	−63.1831	26.95	26.05	1,294	1
Caryoborus serripes	Bolivia	−11.1172	−66.1239	26.52	25.32	1,651	1
Caryoborus serripes	Brazil	−3.1033	−60.0114	27.45	26.98	2,153	1
Caryoborus serripes	Brazil	−14.7864	−39.2728	24.33	22.88	1,445	5
Caryoborus serripes	Brazil	−18.5833	−39.7500	24.07	22.02	1,307	5
Caryoborus serripes	Brazil	−19.3936	−40.0581	24.27	22.08	1,203	1
Caryoborus serripes	Brazil	−4.2614	−55.9719	27.35	26.77	2,137	1
Caryoborus serripes	Brazil	−2.4333	−54.7000	26.07	25.45	2,154	1
Caryoborus serripes	Brazil	−22.8750	−43.2775	23.02	20.52	1,256	1
Caryoborus serripes	Brazil	−5.9833	−35.9333	25.09	23.42	539	1
Caryoborus serripes	French Guiana	4.9389	−52.3206	26.54	25.97	3,021	1
Caryoborus serripes	French Guiana	4.5742	−52.2261	25.19	24.68	3,766	1
Caryoborus serripes	French Guiana	4.8167	−53.2667	25.23	24.63	2,664	1
Caryoborus serripes	Guyana	5.2617	−59.1483	26.45	25.65	2,853	1
Caryoborus serripes	Peru	−4.9081	−73.6667	26.83	26.25	2,632	4
Caryoborus serripes	Peru	−4.0536	−73.1700	26.43	25.87	2,716	1
Caryoborus serripes	Peru	−3.9167	−73.7500	26.39	25.80	2,712	4
Caryoborus serripes	Peru	−3.4000	−72.7500	26.23	25.58	2,873	4
Caryoborus serripes	Peru	−6.0333	−76.9667	22.99	22.33	1,392	4
Caryoborus serripes	Peru	−4.9167	−73.6667	26.83	26.25	2,632	4
Caryoborus serripes	Peru	−12.6333	−69.2000	25.51	23.93	2,245	4
Caryoborus serripes	Suriname	4.7711	−55.0494	26.78	26.03	2,313	1
Caryobruchus curvipes	Guatemala	16.9833	−89.8333	25.55	22.95	1,511	1
Caryobruchus curvipes	Guatemala	17.3936	−89.6336	25.78	22.90	1,240	1
Caryobruchus curvipes	Mexico	17.4489	−91.9614	25.39	22.78	2,563	J. Romero Nápoles collections (this paper)
Caryobruchus curvipes	Mexico	16.7500	−93.1000	23.75	21.60	912	1
Caryobruchus curvipes	Mexico	17.2752	−95.0542	25.14	22.20	2,579	G. E. Morse collections (this paper)
Caryobruchus curvipes	Mexico	18.2372	−96.4047	25.20	21.85	2,732	1
Caryobruchus curvipes	Mexico	23.1028	−106.0203	24.75	20.77	834	1
Caryobruchus gleditsiae	Bermuda	32.3475	−64.6633	21.64	17.28	1,513	1
Caryobruchus gleditsiae	Cuba	21.5497	−77.9717	25.10	22.32	1,403	1
Caryobruchus gleditsiae	Cuba	21.3808	−77.9169	25.19	22.45	1,414	1
Caryobruchus gleditsiae	Cuba	23.1319	−82.3642	25.04	22.22	1,238	1
Caryobruchus gleditsiae	Cuba	23.1239	−82.3003	24.85	22.00	1,289	1
Caryobruchus gleditsiae	Jamaica	17.9183	−76.1844	26.60	25.30	1,715	1
Caryobruchus gleditsiae	Mexico	22.3403	−105.2983	24.66	21.27	1,274	1
Caryobruchus gleditsiae	Mexico	22.6578	−105.6069	24.87	21.10	1,021	1
Caryobruchus gleditsiae	Mexico	27.9333	−111.0500	24.66	18.28	191	1
Caryobruchus gleditsiae	Mexico	29.5500	−110.4250	22.33	15.03	460	ASUT (this paper)
Caryobruchus gleditsiae	Mexico	18.9761	−96.0775	25.91	22.65	1,538	1
Caryobruchus gleditsiae	United States	29.6500	−82.3167	20.43	13.30	1,322	1
Caryobruchus gleditsiae	United States	29.5744	−82.3474	20.60	13.50	1,337	G. E. Morse collections (this paper)
Caryobruchus gleditsiae	United States	27.2928	−81.3631	22.34	16.70	1,216	1
Caryobruchus gleditsiae	United States	26.4328	−81.8156	23.26	18.13	1,336	1

Table S4. Cont.

Species	Country	Latitude	Longitude	MAT	CQMT	MAP	Source
Caryobruchus gleditsiae	United States	29.1667	−81.8000	20.95	14.25	1,287	1
Caryobruchus gleditsiae	United States	25.6769	−80.2719	24.13	20.00	1,295	1
Caryobruchus gleditsiae	United States	25.4475	−80.4794	23.71	19.40	1,506	1
Caryobruchus gleditsiae	United States	25.4683	−80.4778	23.64	19.33	1,537	1
Caryobruchus gleditsiae	United States	25.4045	−80.6925	23.67	19.30	1,394	G. E. Morse collections (this paper)
Caryobruchus gleditsiae	United States	24.7167	−81.0833	24.67	20.67	1,102	1
Caryobruchus gleditsiae	United States	28.5333	−81.3667	22.03	15.87	1,258	1
Caryobruchus gleditsiae	United States	27.7456	−81.5308	22.41	16.60	1,249	1
Caryobruchus gleditsiae	United States	25.9014	−97.4972	23.21	16.57	687	1
Caryobruchus gleditsiae	United States	26.2000	−98.2167	23.27	15.77	558	1
Caryobruchus marieae	Cuba	23.1319	−82.3642	25.04	22.22	1,238	1
Caryobruchus maya	Guatemala	17.2250	−89.6133	25.26	22.45	1,339	1
Caryobruchus maya	Mexico	18.5339	−89.6408	25.08	21.90	1,121	1
Caryobruchus maya	Mexico	18.5169	−89.3958	24.63	21.48	1,137	1
Caryobruchus maya	Mexico	18.2453	−92.8314	26.51	23.75	1,872	1
Caryobruchus maya	Mexico	19.7997	−87.4764	26.06	23.65	1,252	1
Caryobruchus maya	Mexico	19.2153	−88.1011	25.87	23.43	1,275	1
Caryobruchus maya	Mexico	18.4861	−88.8217	25.05	22.50	1,321	1
Caryobruchus maya	Mexico	18.3817	−88.5658	25.08	22.87	1,359	1
Caryobruchus maya	Mexico	20.9947	−89.6086	25.78	22.98	950	1
Caryobruchus rubidus	Mexico	16.7500	−93.1000	23.75	21.60	912	J. Romero Nápoles collections (this paper)
Caryobruchus rubidus	Mexico	17.9824	−96.1100	25.00	21.62	2,777	G. E. Morse collections (this paper)
Caryobruchus rubidus	Mexico	18.3650	−95.7953	26.27	23.00	1,558	1
Caryobruchus rubidus	Mexico	18.4442	−95.2133	24.37	21.27	2,157	1
Caryobruchus veseyi	Mexico	29.7294	−114.7208	18.16	13.05	115	1
Caryobruchus veseyi	Mexico	23.7000	−109.8167	21.57	16.25	378	1
Pachymerus abruptestriatus	Brazil	−15.2333	−39.6167	22.17	20.43	1,067	1
Pachymerus bactris	Brazil	−3.1033	−60.0114	27.45	26.98	2,153	1
Pachymerus bactris	Ecuador	−2.4581	−79.2614	23.87	22.93	1,943	1
Pachymerus bactris	French Guiana	5.1597	−52.6503	26.06	25.62	2,855	1
Pachymerus bactris	Panama	9.1667	−79.8333	26.58	25.80	2,682	1
Pachymerus bactris	Panama	8.9000	−79.5833	26.94	26.43	1,844	1
Pachymerus bactris	Panama	8.8064	−79.5167	26.98	26.50	1,717	1
Pachymerus bactris	Venezuela	10.2469	−67.5961	24.98	24.17	932	1
Pachymerus bactris	Venezuela	10.4000	−66.9000	19.53	18.33	1,084	1
Pachymerus bridwelli	Argentina	−28.5000	−59.0500	20.80	15.52	1,063	1
Pachymerus bridwelli	Argentina	−31.3869	−58.0200	18.63	12.98	1,277	1
Pachymerus bridwelli	Argentina	−32.2667	−68.4167	17.69	9.70	150	1
Pachymerus bridwelli	Argentina	−25.2833	−57.7167	23.24	18.58	1,375	6
Pachymerus bridwelli	Argentina	−25.1600	−58.1464	22.66	18.10	1,124	1
Pachymerus bridwelli	Argentina	−25.7050	−54.2483	20.13	15.63	1,767	1
Pachymerus cardo	Bolivia	−14.2333	−63.5167	25.50	23.72	1,458	1
Pachymerus cardo	Brazil	−2.0500	−59.9000	26.84	26.45	2,802	7
Pachymerus cardo	Brazil	−22.9675	−43.2239	22.53	20.08	1,401	1
Pachymerus cardo	Brazil	3.4167	−61.6667	26.69	25.95	1,760	8
Pachymerus cardo	Colombia	3.5394	−76.3036	23.93	23.58	1,026	1
Pachymerus cardo	Colombia	4.1267	−76.3706	21.36	20.98	1,463	1
Pachymerus cardo	Colombia	4.6647	−76.0486	23.28	22.82	1,332	1
Pachymerus cardo	Colombia	3.3753	−76.5336	23.98	23.48	1,307	G. E. Morse collections (this paper)
Pachymerus cardo	Costa Rica	11.2178	−85.6125	26.31	25.38	2,149	1
Pachymerus cardo	French Guiana	4.8167	−53.2667	25.23	24.63	2,664	1
Pachymerus cardo	Guyana	6.2800	−57.5753	27.16	26.77	1,156	1
Pachymerus cardo	Guyana	6.8064	−58.1453	26.85	26.42	2,335	1
Pachymerus cardo	Honduras	15.7000	−86.8500	24.35	22.23	2,121	2
Pachymerus cardo	Honduras	15.7667	−87.0000	26.46	24.45	2,569	2
Pachymerus cardo	Panama	9.1667	−79.8333	26.58	25.80	2,682	1
Pachymerus cardo	Panama	9.0000	−79.7500	26.39	25.70	2,363	1
Pachymerus cardo	Panama	8.8792	−79.7822	26.77	26.23	2,003	1

Table S4. Cont.

Species	Country	Latitude	Longitude	MAT	CQMT	MAP	Source
Pachymerus cardo	Panama	9.0483	−79.6606	26.36	25.65	2,183	1
Pachymerus cardo	Panama	9.0833	−79.6167	26.35	25.65	2,099	1
Pachymerus cardo	Panama	9.0333	−79.6333	26.35	25.70	2,190	1
Pachymerus cardo	Panama	9.0933	−79.6516	25.99	25.23	2,292	G. E. Morse collections (this paper)
Pachymerus cardo	Panama	9.0618	−79.6437	26.36	25.65	2,183	G. E. Morse collections (this paper)
Pachymerus cardo	Peru	−4.9081	−73.6667	26.83	26.25	2,632	4
Pachymerus cardo	Peru	−3.9167	−73.7500	26.39	25.80	2,712	4
Pachymerus cardo	Peru	−4.9167	−73.6667	26.83	26.25	2,632	4
Pachymerus cardo	Peru	−12.6333	−69.2000	25.51	23.93	2,245	4
Pachymerus cardo	Trinidad and Tobago	10.6667	−61.5167	25.72	24.83	1,861	1
Pachymerus cardo	Trinidad and Tobago	10.6636	−61.5267	26.57	25.72	1,618	1
Pachymerus cardo	Venezuela	10.2469	−67.5961	24.98	24.17	932	1
Pachymerus cardo	Venezuela	8.4258	−70.6281	26.83	26.47	1,772	1
Pachymerus cardo	Venezuela	10.1117	−68.0653	24.56	24.08	1,233	1
Pachymerus cardo	Venezuela	10.4000	−66.9000	19.53	18.33	1,084	1
Pachymerus cardo	Venezuela	8.8041	−65.2019	26.92	26.42	1,221	G. E. Morse collections (this paper)
Pachymerus cardo	Venezuela	8.9333	−67.4167	27.38	26.43	1,196	1
Pachymerus cardo	Venezuela	8.4822	−72.3317	28.10	27.30	2,285	1
Pachymerus cardo	Venezuela	9.8753	−70.9619	27.73	27.23	1,402	1
Pachymerus nucleorum	Bolivia	−17.4500	−63.6667	24.13	20.97	1,572	CAS (this paper)
Pachymerus nucleorum	Brazil	−12.9742	−38.5133	25.12	23.55	1,834	1
Pachymerus nucleorum	Brazil	−21.7000	−57.8667	25.08	21.12	1,284	1
Pachymerus nucleorum	Brazil	−10.8125	−50.6189	27.39	26.43	1,812	CAS (this paper)
Pachymerus nucleorum	Paraguay	−23.4308	−56.4989	22.91	19.07	1,427	G. E. Morse collections (this paper)
Pachymerus sveni	Brazil	−3.1033	−60.0114	27.45	26.98	2,153	1
Pachymerus sveni	Brazil	−3.9164	−38.6075	25.77	25.00	1,406	1
Pachymerus sveni	Brazil	−1.4372	−48.4706	26.88	26.45	2,438	1
Pachymerus sveni	Brazil	−22.8750	−43.2775	23.02	20.52	1,256	1
Pachymerus sveni	Brazil	−28.4000	−54.9667	20.68	15.72	1,901	1
Pachymerus sveni	Venezuela	10.4000	−66.9000	19.53	18.33	1,084	1
Pachymerus thoracicus	Paraguay	−25.2833	−57.6333	23.30	18.67	1,403	6
Pachymerus undetermined species	Paraguay	−25.5100	−57.5600	22.87	18.23	1,388	G. E. Morse collections (this paper)
Pachymerus undetermined species	Paraguay	−23.3442	−57.0442	23.46	19.30	1,348	G. E. Morse collections (this paper)
Speciomerus giganteus	Brazil	−17.8872	−51.7181	23.52	21.70	1,535	1
Speciomerus giganteus	Brazil	−2.9381	−51.8617	26.65	26.20	2,067	1
Speciomerus giganteus	Colombia	8.9833	−73.9667	28.43	27.87	2,086	1
Speciomerus giganteus	Costa Rica	10.0631	−84.7700	26.81	25.92	1,872	1
Speciomerus giganteus	Panama	9.1667	−79.8333	26.58	25.80	2,682	1
Speciomerus giganteus	Panama	9.3728	−79.8811	26.74	26.10	3,256	CAS (this paper)
Speciomerus giganteus	Panama	9.1317	−79.7769	26.41	25.57	2,497	1
Speciomerus giganteus	Paraguay	−25.5333	−57.0500	21.48	17.17	1,453	G. E. Morse collections (this paper)
Speciomerus giganteus	Paraguay	−23.4308	−56.4989	22.91	19.07	1,427	G. E. Morse collections (this paper)
Speciomerus giganteus	Peru	−3.9167	−73.7500	26.39	25.80	2,712	4
Speciomerus giganteus	Peru	−4.9167	−73.6667	26.83	26.25	2,632	4
Speciomerus revoili	Paraguay	−24.1500	−55.7000	22.57	18.47	1,550	G. E. Morse collections (this paper)
Speciomerus revoili	Paraguay	−25.5333	−57.0500	21.48	17.17	1,453	G. E. Morse collections (this paper)
Speciomerus rubrofemoralis	Brazil	−17.8872	−51.7181	23.52	21.70	1,535	1
Speciomerus rubrofemoralis	Brazil	−15.4333	−55.7500	22.87	20.88	1,548	1
Speciomerus rubrofemoralis	Brazil	−16.4681	−54.6414	24.93	22.35	1,523	1
Speciomerus ruficornis	Brazil	−2.8333	−55.1333	26.15	25.68	1,957	1
Speciomerus ruficornis	Brazil	−15.4333	−55.7500	22.87	20.88	1,548	1
Speciomerus ruficornis	Brazil	−12.7667	−55.6000	24.95	23.63	1,852	1

Table S4. Cont.

Species	Country	Latitude	Longitude	MAT	CQMT	MAP	Source
Speciomerus ruficornis	Paraguay	−23.4308	−56.4989	22.91	19.07	1,427	G. E. Morse collections (this paper)
Speciomerus undetermined species	Paraguay	−25.3500	−57.5167	22.63	18.10	1,408	G. E. Morse collections (this paper)
Speciomerus undetermined species	Paraguay	−23.3442	−57.0442	23.46	19.30	1,348	G. E. Morse collections (this paper)
Caryobruchus gleditsiae	Dominican Republic	18.8300	−69.8000	25.89	24.10	1,946	1
Caryobruchus gleditsiae	Mexico	21.9100	−99.3000	22.40	17.48	1,339	GBIF
Caryobruchus gleditsiae	Mexico	22.3600	−105.0000	23.62	20.22	1,304	GBIF
Caryobruchus gleditsiae	United States	25.8500	−97.4000	23.19	16.60	687	GBIF
Caryobruchus gleditsiae	United States	26.3300	−98.2000	23.08	15.48	584	GBIF
Caryobruchus gleditsiae	United States	28.4300	−99.7000	21.93	13.00	555	GBIF
Caryobruchus gleditsiae	United States	28.8800	−97.9000	20.97	12.30	739	GBIF
Caryobruchus gleditsiae	United States	29.4200	−98.4000	20.65	12.02	697	GBIF
Caryobruchus gleditsiae	United States	29.4500	−98.5000	20.70	12.03	688	GBIF
Caryobruchus gleditsiae	United States	27.2900	−81.3000	22.37	16.72	1,220	GBIF
Caryobruchus gleditsiae	United States	28.1200	−80.6000	22.33	16.77	1,246	GBIF
Caryobruchus marieae	Colombia	4.7400	−76.1000	19.07	18.65	1,880	GBIF
Pachymerus sp.	Brazil	−3.1100	−60.0000	27.45	26.98	2,153	GBIF
Pachymerus cardo	Brazil	−19.5000	−40.6000	24.32	22.20	1,170	GBIF
Pachymerus cardo	Colombia	3.5390	−76.3000	23.93	23.58	1,026	GBIF
Pachymerus cardo	Colombia	4.1260	−76.3000	22.88	22.45	1,236	GBIF
Pachymerus cardo	Colombia	4.7400	−76.1000	19.07	18.65	1,880	GBIF
Pachymerus cardo	Venezuela	8.1590	−70.2000	27.69	27.37	1,535	GBIF
Speciomerus giganteus	Costa Rica	10.8364	−85.6155	24.92	24.08	1,725	GBIF
Speciomerus giganteus	Costa Rica	10.8563	−85.6119	24.92	24.08	1,725	GBIF
Speciomerus giganteus	Costa Rica	10.9625	−85.4953	21.73	20.88	2,723	GBIF
Speciomerus giganteus	Costa Rica	10.5848	−83.5292	26.33	25.42	5,033	GBIF
Speciomerus giganteus	Costa Rica	10.5396	−83.5065	26.25	25.35	4,701	GBIF
Speciomerus giganteus	Costa Rica	8.7594	−83.2831	26.21	25.38	4,840	GBIF
Speciomerus giganteus	Costa Rica	9.3877	−84.1328	26.36	25.50	3,758	GBIF
Speciomerus giganteus	Costa Rica	9.7675	−84.6081	26.31	25.47	2,587	GBIF
Speciomerus giganteus	Costa Rica	9.7742	−84.6081	26.31	25.47	2,587	GBIF
Speciomerus giganteus	Costa Rica	8.6791	−83.5667	25.25	24.40	3,826	GBIF

Decimal latitude and longitudes used. Climate analysis performed using DIVA-GIS software with the WorldClim dataset (9, 10).

1. Nilsson JA, Johnson CD (1993) A taxonomic revision of the palm bruchids (Pachymerini) and a description of the world genera of Pachymerinae. *Mem Am Entomol Soc* 41:1–104.
2. Turnbow RH, Cave RD, Kingsolver JM (2003) An annotated checklist of the Bruchidae of Honduras. *Ceiba* 44(2):269–278.
3. Bridwell JC (1929) A preliminary generic arrangement of the palm bruchids and allies (Coleoptera) with descriptions of new species. *Proc Entomol Soc Wash* 31(8):141–160.
4. Delobel A, Couturier G, Kahn F, Nilsson JA (1995) Trophic relationships between palms and bruchids (Coleoptera: Bruchidae: Pachymerini) in Peruvian Amazonia. *Amazoniana* 13(3-4): 209–219.
5. Silva P (1977) Correcoes e aditamentos ao "Quarto catalogo dos insetos que vivem nas plantas do Brasil" (Coleoptera, Bruchidae, Pachymerinae). *Rev Bras Entomol* 21(1):1–5.
6. Prevett PF (1966) A new genus and species of Pachymerinae (Coleoptera: Bruchidae) from South America. *Proc R Entomol Soc Lond* 35(5-6):81–83.
7. Delgado C (2002) The relationship between *Pachymerus cardo* (Fåhraeus) (Coleoptera: Bruchidae) and the palm *Orbignya spectabilis* (C. martius) Burret (Arecaceae: Cocoeae) in a terra firme forest, Brazilian Amazon. *Amazoniana* 17(1-2):169–171.
8. Silvius KM, Fragoso JMV (2002) Pulp handling by vertebrate seed dispersers increases palm seed predation by bruchid beetles in the northern Amazon. *J Ecol* 90(6):1024–1032.
9. Hijmans RJ, Cameron SE, Parra JL, Jones PG, Jarvis A (2005) Very high resolution interpolated climate surfaces for global land areas. *Int J Climatol* 25(15):1965–1978.
10. Hijmans RJ, et al. (2013) WorldClim - Global Climate Data/DIVA-GIS. Available at www.worldclim.org. Accessed April 2, 2013.